A simple levitated-drop tensiometer

J. Arcenegui-Troya,[1] A. Belman-Martínez,[2] A.A. Castrejón-Pita,[1] and J.R. Castrejón-Pita[2]

[1]*Department of Engineering Science, University of Oxford, Oxford OX1 3PJ, UK*
[2]*School of Engineering and Materials Science, Queen Mary, University of London, E1 4NS, UK*

A reliable, simple and affordable liquid tensiometer is presented in this paper. The instrument consists of 72 ultrasonic transmitters in a *tractor beam* configuration that levitates small liquid samples (droplets) in air. Under operation, the instrument imparts a pressure instability that causes the droplet to vibrate while still levitating. Droplet oscillations are then detected by a photodiode and the signal recorded by an oscilloscope. The frequency these oscillations are obtained and then used to obtain the effective surface tension of the sample. The instrument operates at the millisecond scale time (t <12.5 ms), with very small liquid volumes ($\sim$ 0.5 μl), and the sample is recoverable after testing. The instrument has been experimentally validated with acetone, ethanol, fluorinert FC-40, water and whole milk.

PACS numbers: 47.55.D-, 47.55.db, 47.55.df

I. INTRODUCTION

Liquid characterisation is important in a vast range of industrial processes. In inkjet and spray applications, ink and fluid properties determine the size and speed of droplets, and control the printing and coating performance [1]. In nature, liquid properties determine a plethora of processes ranging from mist formation to spray combustion [2]. In the general context of drop formation, liquid surface tension and viscosity are known to determine whether a liquid filament will break or not into droplets [3, 4].

Various techniques exist to measure liquid properties, each offering advantages and disadvantages depending on the specific application. The simplest way to measure the surface tension of a liquid is thorough the well-known ring and/or plate method, where the force required to break free a metallic ring wetting a liquid surface is measured. In this setup, surface tension is simply obtained from the measured force and the length of the ring. There is also the well-known pendant drop technique, in which experimentally obtained drop shapes are matched with theoretical profiles using the so-called axisymmetric drop shape analysis (ADSA), [5–7]. Another common method to measure surface tension is by sensing the pressure required to form a bubble within a liquid [8]. This method is particularly useful as bubbles can be produced at various rates (the so-called 'bubble-lifetime') in such a way that the surface tension can be recorded at various time scales (or surface ages). These methods are reliable and simple, but they typically require liquid volumes in the order of tens of millilitres to operate, and often work on time scales > 15 ms and some kind of physical contact with part of the instrument (ring, plate, capillary or holder) is normally needed, introducing unnecessary channels for contamination.

A recently developed method to measure liquid properties during inkjet processes consists of analysing the oscillation of ink droplets during the jetting and flight stages of printing via high speed imaging [9, 10]. This method was designed to work under normal printing operational conditions, where drop sizes are of the order of 50 μm in diameter at shear rates of 10^5 s^{-1}. The motivation behind this method was to be able to extract the 'actual' liquid properties under conditions (i.e. shear rates and speeds) relevant to the jetting process for further ink formulation and development. However, most printers (or droplet generators) require several millilitres of ink to operate [10, 15], and therefore the technique is not appropriate for applications where the available liquid volume is limited. In addition, this method is inherently expensive as it requires high-priced microscopes/lenses, high speed cameras, and cumbersome illumination systems. In [11] a simple single-beam optical trapping system is used to study resonant modes of capillary waves in micron-sized aerosol droplets. By analysing the frequency shift power spectrum of light passing through the droplet and extracting peaks in frequency (resonant-modes) the surface tension of such droplets is obtained. Bzdek *et al* [12] extract values for the liquid surface tension of liquids by analysing the oscillations excited after the controlled coalescence of two optically-trapped (holographic optical tweezers) microscopic aerosol droplets. While these optical methods give excellent results, they involve hugely expensive equipment and require a system to generate such diminutive droplets, like in the inkjet methods described above. In contrast, in [13, 14] large (20mm in diameter) water droplets are levitated using a superconducting-solenoid magneto-gravitational potential trap for which values of the surface tension are extracted by studying shape oscillations and analysing frequency peaks in the power spectrum plot. A comparable method that only requires a single droplet of millimetre-sized drops to obtain liquid properties was recently presented in by Kremer et

Please address all correspondence to: jjarcenegui@gmail.com or castrejon@cantab.net

al. [16]. This setup consists of an acoustic levitator that confines and forces oscillations on a liquid drop by varying the perturbation frequency and detecting favourite oscillation modes. Viscosity and surface tension are obtained from the analysis of the oscillations recorded by high speed imaging. Kremer et al. [16] used the classical transmitter-reflector configuration to create a stationary acoustic wave where droplets can be trapped and manipulated at the nodes. Here, we present an alternative technique, also based on the detection of oscillations of acoustically trapped liquid droplets, to optically measured the surface tension of the liquid sample. Our method requires a small liquid volume; a droplet of approximately 1.0 mm in diameter or a volume of 0.5 μl. The major difference between the system presented in this manuscript and the latter is that the droplet oscillations are recorded solely by a photodiode. The photodiode avoids the use of a high-speed camera and microscope lenses thus significantly reducing the cost of the setup without compromising accuracy (a camera setup is also used here for validation only). Droplets are confined by an inexpensive acoustic *tractor-beam* [17], and made to oscillate by momentarily and controllably turning off the acoustic field. A simple lens projects the image of the droplet onto the photodiode in such a way that the amount of light received at the sensor depends on the cross-sectional area of the droplet. These changes on the cross-sectional result in variations of the output voltage of the photodiode from which one can estimate the surface tension.

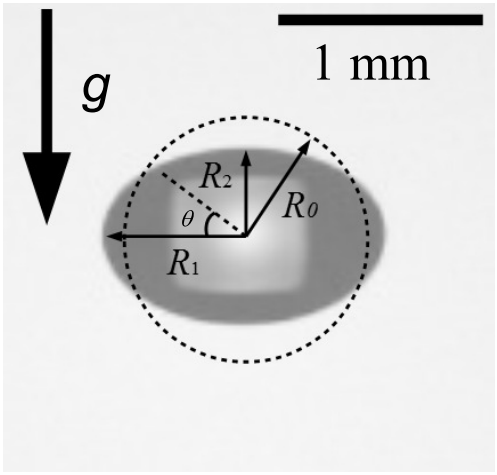

FIG. 1: Snapshot of an oscillating droplet, R_0 is the unperturbed radius and R_1 and R_2 are the semi-axes of the ellipse, which vary with time as the droplet oscillates.

II. THEORETICAL DESCRIPTION

According to Rayleigh [18], the shape of a droplet undergoing axisymmetric oscillations can be expressed in terms of Legendre polynomials P_n, i.e:

$$R(\theta,t) = R_0\left[1+\sum_{n=2}^{\infty} a_n(t)P_n(\cos\theta)\right],$$

where $a_n(t)$ is the amplitude of the n-th oscillation mode, R_0 is the unperturbed radius of the droplet, and θ is the polar angle in spherical coordinates [15]. For small-amplitude oscillations of inviscid liquids, $a_n(t)$ can be described by:

$$a_n(t) \sim \exp(-t/\tau_n)\cos(\Omega_n t),$$

where the oscillation decay time, τ_n, is given by:

$$\tau_n = \frac{\rho R_0^2}{\mu(n-1)(2n+1)}, \tag{1}$$

and its frequency, Ω_n, is

$$\Omega_n^2 = n(n-1)(n+1)\frac{\sigma}{\rho R_0^3} - \left[(n-1)(2n+1)\frac{\mu}{\rho R_0^2}\right]^2, \tag{2}$$

where ρ is the density, μ the dynamic viscosity, and σ the surface tension of the liquid, [19]. Equations 1 and 2 are only valid for low Ohnesorge numbers (Oh$<$ 0.1), where $\mathrm{Oh} = \mu/\sqrt{\rho\sigma R_0}$ [20]. Accordingly, our experimental conditions were kept at Oh < 0.05. In addition, we can safely assume that the fundamental mode ($n = 2$) dominates the droplet dynamics as the amplitude of oscillations were kept below $0.2R_0$, [21]. We consider that effects due to gravity are negligible. Simplifying:

$$R_1(t) = R_0\left[1 + C\exp(-t/\tau_2)\cos(\Omega_2 t)\right], \tag{3}$$

where C is a constant, the decay time is

$$\tau_2 = \frac{\rho R_0^2}{5\mu}, \tag{4}$$

and the frequency of oscillation is

$$\Omega_2^2 = \frac{6\sigma}{\rho R_0^3} - \left[\frac{5\mu}{\rho R_0^2}\right]^2. \tag{5}$$

Under the conditions of our experiments, the second term on the right-hand side is two orders of magnitude smaller than the second term, and is therefore ignored leading to:

$$\Omega_2^2 \simeq \frac{6\sigma}{\rho R_0^3}. \tag{6}$$

In fact, equations 4 and 6 have been used in the past to determine both the viscosity and the surface tension of drops undergoing oscillations following jetting from a inkjet printing nozzle [10, 15]. In the scheme presented here, the oscillation frequency Ω_2 of levitated liquid droplets can be optically detected. The method assumes that the undisturbed droplet radius R_0 can be extracted from a snapshot, or determined from its weight

(assuming that the density is known). The main source of of uncertainty for the surface tension is the uncertainty on the radius of the droplet. In our case, where the radius was determined from a snapshot, the uncertainty on the radius is ± 0.03 mm, what corresponds to 1 pixel.

In our experimental setup, droplet oscillations are recorded as an electric potential (voltage) variation by the oscilloscope. This voltage can readily be related to oscillations on the radii as required by our equations. The cross-sectional area A_D of the droplet, assuming an elliptical shape, projected on the photodiode is expressed as (see Figure 1):

$$A_D = \pi R_1 R_2, \tag{7}$$

where R_1 and R_2 determine the droplet volume, i.e

$$Volume_D = \frac{4}{3}\pi {R_1}^2 R_2 = \frac{4}{3}\pi {R_0}^3. \tag{8}$$

Combining Eqns. 3, 7, and 8 we obtain:

$$A_D = \frac{\pi R_0^2}{1 + C\exp(-t/\tau_2)\cos(\Omega_2 t)}. \tag{9}$$

During experiments the output voltage of the photodiode, V_{out}, is proportional to the active area of the sensor, A_{cell}, that is receiving light. As the drop is located between the light source and the photodiode, its shadow (equivalent to that of the cross-sectional area of the drop) will be projected onto the surface of the photodiode. Consequently, the output voltage, V_{out}, from the photodiode will be proportional to the illuminated are:

$$V_{out} \propto [A_{cell} - A_D]. \tag{10}$$

Here, it is important to note that the size of the droplet's image at the photodiode must be smaller than the sensing area. Finally, combining equations. 9 and 10 we obtain

$$V_{out} = kA_{cell} - \frac{k\pi R_0^2}{[1 + C\exp(-t/\tau_2)\cos(\Omega_2 t)]}, \tag{11}$$

where k is a constant, which depends on the characteristics of the photodiode. In our case, $k = 6.1 \pm 0.5 \cdot 10^7$ V/m^2. Equation 12 indicates that the frequency of oscillation detected by the photodiode is the frequency of droplet oscillations, in Section IV this was confirmed experimentally.

III. EXPERIMENTAL DESCRIPTION

Our experimental setup consists of a *tractor beam* levitator consisting of an array of 72 ultrasonic transmitters (40 kHz) placed in a two-spherical cap configuration (each with 36 transmitters) [17]. Each cap is driven by a 40 kHz signal with a phase difference of 180 from each other. The lower cap contains a central hole to permit the recovery of droplets after use. A diagram of the experimental setup is shown in Figure 2. In this configuration, a standing acoustic wave is created between the caps, with alternating nodes of maximum and minimum pressure. The droplets were trapped and remain levitated in the regions of minimum pressure. The system is driven by a function generator providing a 40 kHz square wave. This signal is then amplified to 25 V, and divided into two 180 degree phased drivers by a L298N power circuit. Oscillations are generated by gating off (controllably switched off by a time w) the driving signal using a pulse generator (TTi GP110), in such a way that the signal is stopped for a short time allowing the droplet to fall and oscillate. In our configuration, for ≈ 1.0 mm droplets, gate times $\Delta < 14$ ms kept the droplet levitating while showing clear oscillations; longer gated times cause the droplet to escape from the node's trapping region. Droplets were levitated at the mid-point in between the caps where the pressure field is the strongest by using a 200 μm superhydrophobic metallic tip syringe. The droplets, while trapped, acquire an ellipsoidal shape due to the acoustic field pressure. During the gate time, the acoustic field stops momentarily, allowing for the restoring force, due to the surface tension alone, to induce oscillations. The liquid sample is readily recoverable by simply switching off the acoustic field, as the drop falls into a container located at the centre of the lower cap.

A 10 W LED cold white light source, coupled to an optical diffuser were used to produce a uniform background for black-light illumination. The image of the droplet was projected onto a Thorlabs PDA100A2 photosensor through a bi-convex lens with a focal distance of $f = 75.6$ mm. Optical distances were adjusted in such a way to generate and image on the sensor with a radius of ≈ 1.54 mm, which covered approximately 10% of total area of the active surface of the photosensor. The acquisition of the signal was triggered by the same pulse generator (TTi GP110) used to gate the signal. The signal from the photodiode was visualised and acquired by a digital oscilloscope Lecroy DO4024. In our analysis routine, the photodiode signal was fitted, using OriginPro 9.0, to the curve given by:

$$V_{out} = A - \frac{B}{1 + C\exp(-t/D)\cos(\pi t/E)}, \tag{12}$$

where A, B, C, D and E are fitting constants. The angular frequency is readily obtained from the constant E. An alternative (faster) method is to apply a Fast Fourier transform to the photodiode signal and obtaining the oscillating frequency Ω_2. However, given the small number of detectable droplet oscillations, this method might result in a poor estimate of the frequency. A comparison between these two methods is seen in Table I for a milk droplet. As observed, within error bars, the results are consistent with each other but the standard error is larger

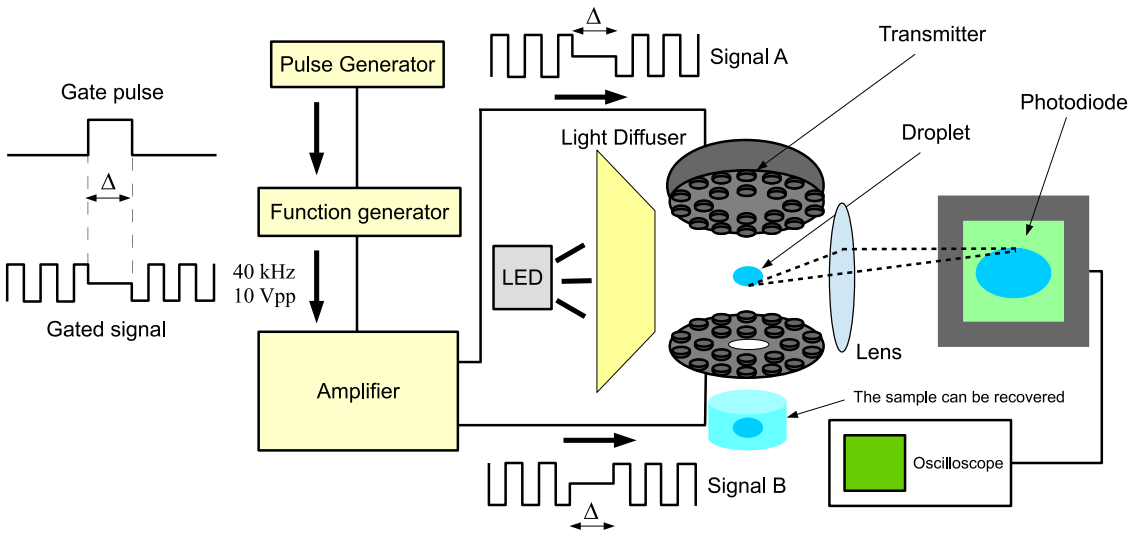

FIG. 2: Experimental setup. Two

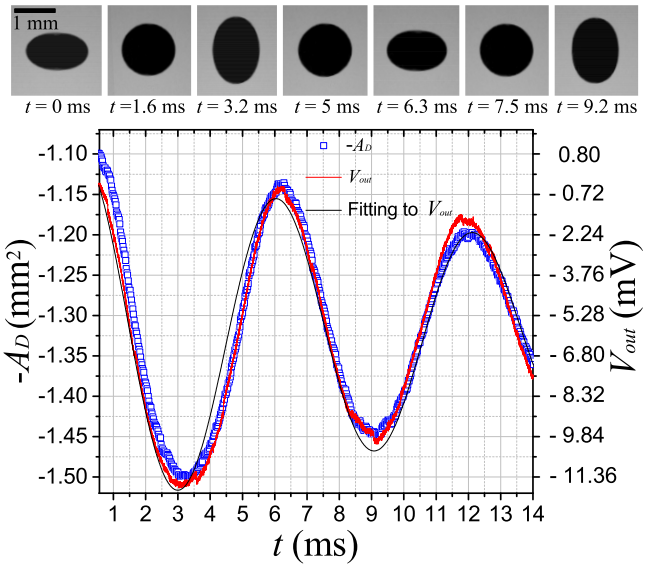

FIG. 3: Colour online. Top: Oscillations of a droplet of whole milk ($R_0 = 0.66$ mm) at different times as captured by high-speed imaging. The graph shows the droplet area measurements (in blue), the output voltage from the photodiode (in red), and a damped sinusoidal fitting. For this particular experiment, the gate time was of $\Delta = 14.0$ ms.

for the FFT method.

In addition, Fig. 3 contrasts the measurement of the liquid surface tension using the fitting method with that obtained by the shadowgraphy-based high-speed imaging scheme presented in [16]. Figure 3 shows a time-sequence of images showing the droplet oscillations as recorded by a high speed camera (Phantom M310), and an example signals obtained by both the photodiode and high-speed methods applied to an oscillating droplet of milk. Standard values for surface tension of the working fluids were taken from the literature and also measured in the laboratory using a Sita Pro-line t15 tensiometer [22–25].

Ω_2 (Hz) FFT	Ω_2 (Hz) from fitting	$\bar{\sigma}$ (mN/m) FFT	$\bar{\sigma}$ (mN/m) from fitting
1082 ± 44	1039 ± 4	53 ± 6	50.0 ± 1.3

TABLE I: Comparison of results obtained from the fitting and the FFT of the signal for a milk droplet of diameter $R_0 = 0.65 \pm 0.03$ mm.

The radius of the spherical droplet was computed from a snapshot of the droplet at equilibrium (rest). The shape of the droplet in this state is that of an oblate spheroid; from these snapshots we were able to determine its axes and thus its volume. The radius of the equivalent spherical droplet was then worked out from this volume. Given the resolution of our camera, the error in the measurement of the axes was of ±1 pixel which leads to an error of 0.03 mm on the radius.

IV. RESULTS

High-speed imaging was carried out simultaneously to photodiode measurements to confirm that equations 9 and 12 yield correct results. Images from a high-speed camera, taken at 56,000 frames per second, of oscillating milk droplets were analysed through image analysis (using a Matlab code developed in-house) to extract the area of the droplet for each frame. Figure 3 shows the droplet area A and the photodiode signal. As seen, both results are consistent. Milk was chosen for validation as it is naturally opaque and produces a clear dark image at the surface of the photosensor.

Further experiments with clear liquids demonstrated that the frequency measured by the photodiode accurately follows the droplet's oscillation frequency. Matte

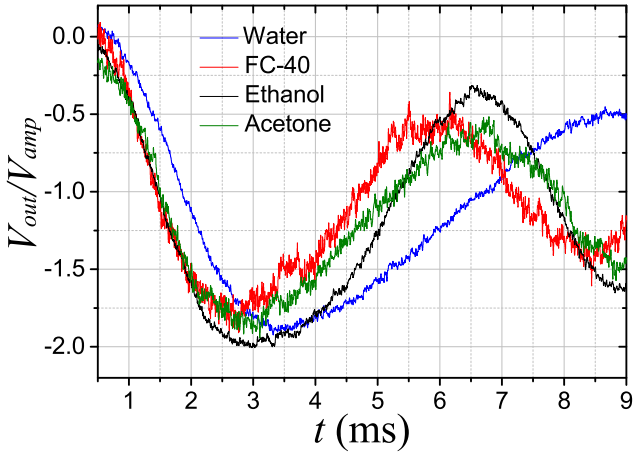

FIG. 4: Droplet oscillations recorded by the oscilloscope for water ($R_0 = 0.9$ mm), ethanol ($R_0 = 0.55$ mm), fluorinert FC-40 ($R_0 = 0.35$ mm) and acetone ($R_0 = 0.57$ mm) droplets. The gate time for all these cases was of $\Delta = 9.5$ ms. The photodiode voltage signal V_{out} have been normalised using its amplitude V_{amp}.

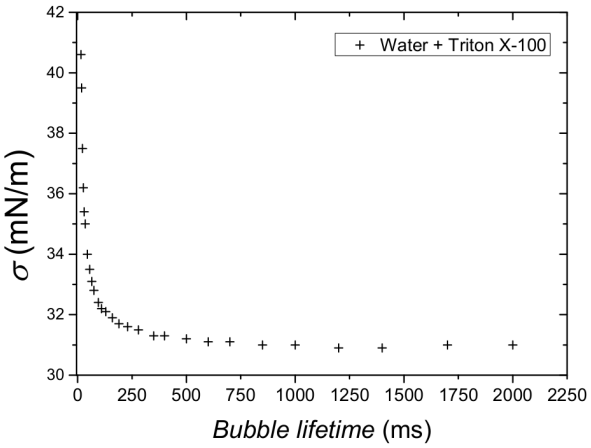

FIG. 5: Dynamic curve of surface tension of a 0.3 wt% Triton X-100 in deionized water for bubble lifetimes ranging from 15ms to 2000ms. The value of the surface tension asymptotically tends towards a value of $\sigma = 31.0 \pm 0.1$ mN/s for long lifetimes.

or opaque fluids provide clean signals as clear liquids, such as water or ethanol, do not form uniform dark (shadow) images on the surface of the photodiode as some refracted light (lensing) can still reach the sensor through the central part of the droplet. Although these signals may be noisier, the presented method is still appropriate to extract surface tension.

Our method was tested with the following fluids: water, Fluorinert (FC-40), ethanol, acetone, milk (whole) and an aqueous solution of Triton X-100. Typical photodiode output signals are shown in Fig. 4 and liquid surface tension measurements are given in Table II together with accepted values found elsewhere [22–25]; as seen, experimental values are consistent with those in the literature. The radii of the droplets were determined via analysis of a snapshot; these values an their uncertainties are also included in the table.

The 'literature' value for FC-40 comes from the datasheet provided by the supplier, Minnesota Mining and Manufacturing Company (3M), while the surface tension for the Water/Triton mixture corresponds to the value found for long (> 1000ms) bubble lifetimes. The uncertainty for each individual value of surface tension has been calculated according to the theory for propagation of uncertainties. The average value is also presented in the table and its error was given by the standard error of these measurements.

As Table II demonstrate, the obtained values for the surface tension agree well with the values found in the literature, for all the fluids used in our tests. For milk, our result is slightly different to the literature value; however, we suspect that these values undoubtedly vary due to the specific brand used, contents, age, etc. The experiments with the Triton surfactant demonstrate that the surface tension value obtained using levitated droplets is that corresponding to the 'static surface tension' as the value found here is consistent to that for long surface ages (i.e. > 1.0 s) as shown in Fig. 5. Here, a bubble-pressure tensiometer was used to determine the dynamic surface tension. This is an expected result, i.e. the droplet is static (trapped in space) and in equilibrium before the perturbation is applied and has therefore reached its static surface tension value. In our method the droplet radii are perturbed by 25% of its original value, which would lead to a change in the surface area (assuming perfect ellipsoids) of less than 8%. Consequently, the expected change in the surface tension due to surface change is negligible and the value we find in our system corresponds (within error) to the dynamic surface tension at long surface lifetimes. The use of Nigrosin as a dye exemplifies the fact that the proposed technique successfully extracts the surface tension regardless of the fluid's optical properties as even the most transparent fluid will refract enough light to project a shadow onto the sensor's surface. Ethanol + dye yields a smaller experimental error as the shadow is better defined and its signal less affected by light lensing through the droplet.

V. CONCLUSIONS

We have developed a technique to optically extract the surface tension of levitating liquid droplets. The technique can accurately determine the surface tension of a variety of fluids, including those with surfactants, and is only limited by the viscosity of the fluids as large viscosities will result in overdamping, for which no oscillations would be observed. Moreover, a quick analysis of the timescales involved in the dynamics (decay time, Equation 4, and oscillation frequency, Equation 5), yields an Oh ≤ 0.25 required in order to

observe at least one characteristic time period of the oscillation during which the initial amplitude decays by a factor of 1/e. This, together with the maximum Oh required by the theoretical treatment to be valid allow us to provide a limit for the droplet's Oh ($\leq$ 0.1) for which this technique would generate accurate results. The maximum Ohnesorge for the experiments presented here is Oh $\approx$ 0.05. By testing the system using the surfactant containing aqueous solution, we further prove the power of the technique to provide the surface tension of fluids equivalent to that of the 'static' condition when using the pendant drop technique or long lifetimes if using the bubble method. The technique is affordable as it does not require a high speed camera, it operates with a very small liquid samples ($\sim$ 0.5 mm in radius) and, moreover, the sample can be recovered after use without the need to be in physical contact with any sensor or probe. A future study could consist of finding a transfer function to convert the oscillations detected by the photosensor (i.e oscillations of the cross-sectional area) into oscillations of the droplet's radius from which one could then also extract the viscosity following the methods used in past works, [10] and [16].

Acknowledgements

This work was financially supported by the Royal Society (URF\R\180016, and RGF\EA\181002), the EPSRC (EP/P024173/1) and by an Equipment Award from the Department of Engineering Science, Oxford.

[1] J Eggers, E Villermaux, Physics of liquid jets, Reports on Progress in Physics, 71, 036601 (2008).

[2] S.T. Thoroddsen, K. Takehara and T.G. Etoh, Micro-splashing by drop impacts, J. Fluid Mech., 707 560-570 (2012).

[3] A.A. Castrejon-Pita, J.R. Castrejon-Pita, I.M. Hutchings, Breakup of liquid filaments, Physical Review Letter, 108, 074506 (2012).

[4] J. Eggers, Drop formation-an overview. Z Angew Math Mech, 85, 400?410 (2005).

[5] F. Bashforth, J.C. Adams, An attempt to test the theories of capillary action. Cambridge University Press, London, England (1883).

[6] Y. Rotenberg, L. Boruvka, A.W. Neumann, Determination of surface tension and contact angle from the shapes of axisymmetric fluid interfaces, Journal of Colloid and Interface Science, 93, 1, pp. 169-183(1983).

[7] Y. Chang, M. Wu, Y. Hung, and S. Lin, Accurate surface tension measurement of glass melts by the pendant drop method. Review of Scientific Instruments 82, 055107 (2011).

[8] V.B. Fainerman, Accurate analysis of the bubble formation process in maximum bubble pressure tensiometry, Rev. Sci. Instrum. 75 213 (2004).

[9] H.J.J. Staat, A. van der Bos, M. van den Berg, H. Reinten, H. Wijshoff, M. Versluis, D. Lohse, Ultrafast imaging method to measure surface tension and viscosity of inkjet-printed droplets in flight, Experiments in fluids, 58, 2 (2017).

[10] S.D. Hoath, W.K. Hsiao, G.D. Martin, S. Jung, S.A. Butler, N.F. Morrison, O. G. harlen, L. S. Yang, C. D. Bain, I. M. Hutchings, Oscillations of aqueous PEDOT: PSS fluid droplets and the properties of complex fluids in drop-on-demand inkjet printing, Proc Royal Soc Lon, 223, 28-36 (2015).

[11] T. Endo, K. Ishikawa, M. Fukuyama, M. Uraoka, S. Ishizaka, and A. Hibara, Spherical Spontaneous Capillary-Wave Resonance on Optically Trapped Aerosol Droplet, Journal of Physical Chemistry C, 122, 20684-20690 (2018).

[12] B. R. Bzdek, R. M. Power, S. H. Simpson, J. P. Reid and C. P. Royall, Precise, contactless measurements of the surface tension of picolitre aerosol droplets Chemical Science, 7, 274 (2016).

[13] R. J. A. Hill and L. Eaves, Vibrations of a diamagnetically levitated water droplet, Physical review E, 81, 056312 (2010).

[14] R. J. A. Hill and L. Eaves, Addendum to 'Vibrations of a diamagnetically levitated water droplet', Physical review E, 85, 017301 (2012).

[15] L. Yang, B.K. Kazmierski, S.D. Hoath, S. Jung, W. Hsiao, Y. Wang, A. Berson, O. Harlen, N. Kapur, and C.D. Bain, Determination of dynamic surface tension and viscosity of non-Newtonian fluids from drop oscillations, Physics of Fluids, 26, 1131-3 (2014).

[16] J. Kremer, A. Kilzer and M. Petermann, Simultaneous measurements of surface tension and viscosity using freely decaying oscillations of acoustically levitated droplets, Review of Scientific Instruments, 89, 015109 (2018).

[17] A. Marzo, S.A. Seah, B.W. Drinkwater, D.R. Sahoo, B. Long, S. Subramanian, Holographic acoustic elements for manipulation of levitated objects, Nature Communications, 6, 8661 (2015).

[18] L. Rayleigh. On the capillary phenomena of jets, Proc Royal Soc Lon, 29, 196-199 (1879).

[19] H. Lamb, On the oscillations of a viscous spheroid, Proc Lond Math Soc, 1, 51 (1881).

[20] A. Prosperetti, Free oscillations of drops and bubbles: the initial-value problem, Journal of Fluid Mechanics, 100, 333-347 (1980).

[21] E. Becker, W.J. Hiller and T.A. Kowalewski, Experimental and theoretical investigation of large-amplitude oscillations of liquid droplet, Journal of Fluid Mechanics, 231, 189 (1991).

[22] A. J. Bertsch, Surface tension of whole and skim-milk between 18 and 135 °C, Journal of Dairy Research, 50, 259-267 (1983).

[23] A. S. Bakshi and D. E. Smith, Effect of Fat Content and Temperature on Viscosity in Relation to Pumping Requirements of Fluid Milk Products, Journal of Dairy Research, 67, 1157-1160 (1984).

[24] G. Vázquez, E. Alvarez and J. M. Navaza, Surface Tension of Alcohol + Water from 20 and 50 °C , Journal of

Chemical Engineering Data, 40, 611-614 (1995).
[25] K. S. Howard and R. A. McAllister, Surface Tension of Acetone-water Solutions Up to Their Normal Boiling Points , AIChE Journal, 3, 325-329 (1957).

Fluid	R_0	Ω_2	$\bar{\sigma}$	σ_{ref}
	mm	Hz	mN/m	mN/m
Water	0.90 ± 0.03	742.7 ± 32.4	71.4 ± 2.2	72.75
FC-40	0.34 ± 0.03	1072.5 ± 126.9	14.4 ± 1.3	16.00
Ethanol	0.59 ± 0.03	920.8 ± 73.1	22.2 ± 1.9	22.31
Acetone	0.56 ± 0.03	1035.3 ± 69.6	24.4 ± 1.0	23.24
Milk	0.65 ± 0.03	1039.0 ± 56.9	50.1 ± 1.3	52.40
Ethanol + dye	0.83 ± 0.03	541.0 ± 23.6	22.2 ± 0.5	22.31
Water + Triton X-100	0.91 ± 0.03	503.6 ± 20.3	31.5 ± 0.7	31.00*

TABLE II: Experimental measurements for the surface tension of various liquids. All measurements were taken at 20 Celsius. The final values represent averages from independent experimental runs with the same droplet diameter. *The reference value σ_{ref} for the water+Triton mixture corresponds to that obtained by the bubble pressure method at a surface lifetime > 1.0 s, please see Figure 5.